31st EPS Conference on Plasma Phys. London, 28 June - 2 July 2004 ECA Vol.**28G**, P-1.053 (2004)

Stimulated scattering instabilities of electromagnetic waves in the Earth's mesosphere

L. Stenflo[1], P. K. Shukla[2], B. Eliasson[3]

[1] *Department of Physics, Umeå University, SE-90187 Umeå, Sweden*

[2,3] *Institut für Theoretische Physik IV, Fakultät für Physik und Astronomie, Ruhr-Universität Bochum, D-44780 Bochum, Germany*

Email: [1]Lennart.Stenflo@physics.umu.se, [2]ps@tp4.rub.de, [3]bengt@tp4.rub.de

Abstract

The nonlinear interaction between intense ordinary mode (O-mode) radio waves and modified magnetosonic waves in partially ionized space dusty plasmas is considered, including the combined action of the radio wave pressure and the electron Joule heating caused by the O-mode electric field. Decay and modulational instabilities are studied by means of a nonlinear dispersion relation.

We consider the parametric coupling between the modified Rao dust magnetoacoustic perturbations [1] and a large amplitude HF radio/radar wave of ordinary polarization in the partially ionized dusty plasmas of the Earth's ionosphere and mesosphere, taking into account the combined effects of the radio/radar wave ponderomotive force and the differential electron Joule heating. Following the standard procedure, we have derived the nonlinear dispersion relation [2] in order to investigate the parametric instabilities of a constant amplitude HF ordinary mode radio/radar pump $A_{z0}\exp(-i\omega_0 t + ik_0 x)$ + complex conjugate. We have

$$\left[(\Omega + i\nu_i)^2 - \Omega_R^2\right]\Omega - (\Omega + i\nu_i)K^2V_R^2 = (\Omega + i\nu_i)\omega_{pi}^2K^2V_0^2\left[1 + i\frac{4\nu_e}{3(\Omega + i\nu_r + i\Omega_\chi)}\right]\sum_{+,-}\frac{1}{D_\pm}, \tag{1}$$

where $\omega_{pi} = (4\pi n_{i0}e^2/m_i)^{1/2}$, $\Omega_\chi = K^2\chi/3n_{e0}$, $V_0^2 = e^2|E_0|^2/4m_e^2\omega_0^2$, $E_0 = \omega_0 A_{z0}/c$, $D_\pm = \pm 2\omega_0(\Omega - KV_g + i\Gamma \mp \delta)$, and $\delta = K^2c^2/2\omega_0$. Here, $\nu_e = \nu_{en} + \nu_{ei}$ and $\nu_i = \nu_{in} + \nu_{en}m_e n_{i0}/m_i n_{e0}$ where ν_{en}, ν_{ei} and ν_{in} is the electron-neutral, electron-ion and ion-neutral collision frequency, respectively, $\nu_r = [\nu_{in}m_i/(m_i + m_n)] + (\nu_{en}m_e/m_n) + 1/3\tau_i$, where τ_i is the relaxation rate due to inelastic collisions between electrons and neutrals, and $\Gamma = \nu_e\omega_p^2/2\omega_0^2$ where $\omega_p = (4\pi n_{e0}e^2/m_e)^{1/2}$. Furthermore, $\chi = \chi_e + n_{e0}\chi_i/n_{i0}$, where χ_e and χ_i are the cross-field electron and ion thermal diffusivities. We also have the modified Alfvén speed $V_R = (n_{i0}/n_{e0})B_0/\sqrt{4\pi n_{i0}m_i}$ and the Rao cutoff frequency

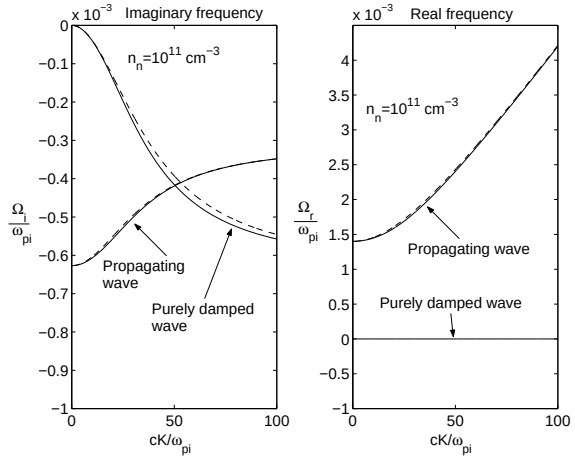

(a) Dispersion curves of Rao's magnetoacoustic waves, depicting the imaginary (left panel) and real (right panel) parts of the frequency as functions of the wavenumber. Exact solutions (solid lines) and approximate solutions (dashed lines).

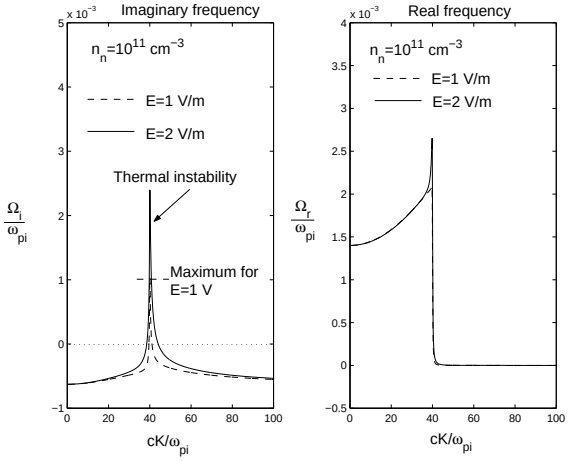

(b) Solutions of the nonlinear dispersion relation (1), depicting the imaginary part (left panel) and real part (right panel) of the frequency as functions of the wavenumber, for the electric pump field $E_0 = 1$ V/m (dashed lines) and $E_0 = 2$ V/m (solid lines).

Figure 1: Dispersion curves, weakly collisional plasma with $n_n = 10^{11}\,\mathrm{cm}^{-3}$.

$\Omega_R = Z_d n_{d0}\omega_{ci}/n_{e0}$ where $\omega_{ci} = eB_0/m_i c$ and Z_d is the number of electrons residing on a dust grain. The remaining symbols are standard.

We have solved the dispersion relation (1) numerically for parameters that are representative of the Earth's ionosphere in the E-region. We then considered a plasma with ion number density $n_{i0} = 1.0 \times 10^5$ cm^{-3}, dust number density $n_{d0} = 950$ cm^{-3}, and $Z_d = 70$, so that $n_{e0}/n_{i0} = 1/3$ and $\omega_{pi} = 7.6 \times 10^4\,\mathrm{s}^{-1}$. We furthermore took the local wavelength of the electromagnetic wave to be $\lambda_0 = 1340$ m, so that $k_0 c/\omega_{pi} = 20$, where $k_0 = 2\pi/\lambda_0$. It then follows that $\omega_p \approx 1.03 \times 10^7$ s^{-1} and $\omega_0 \approx 1.04 \times 10^7$ s^{-1}. We used the magnetic field $B_0 = 0.5$ G, the ion (NO^+) to electron mass ratio $m_i/m_e = 55000$, the neutral to ion mass ratio $m_n/m_i = 1$, and the ion to electron temperature ratio $T_i/T_e = 0.1$, where the electron temperature was $T_e = 3000$ K due to the heating of the electrons by the electromagnetic pump.

We have considered one case in the upper/middle part of the Earth's E-layer for which $n_n = 10^{11}\,\mathrm{cm}^{-3}$, corresponding to a weakly collisional plasma with $\nu_{en} = 3.0 \times 10^3$ s^{-1}, $\nu_{in} = 47$ s^{-1} and $\tau_i = 1.3 \times 10^{-2}$ s, and another case in the lower part of the E-layer with $n_n = 10^{12}\,\mathrm{cm}^{-3}$, corresponding to a strongly collisional plasma with $\nu_{en} = 3.0 \times 10^4$

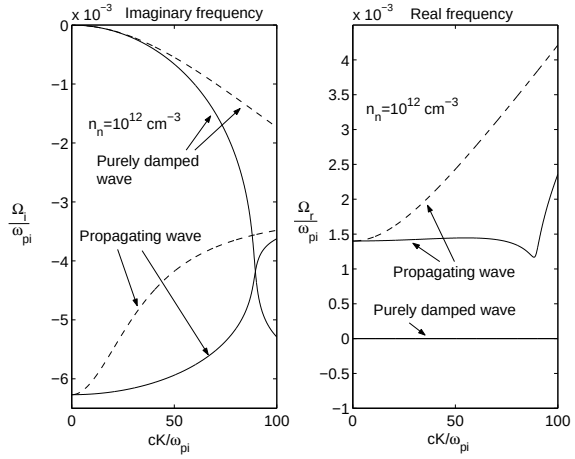

(a) Dispersion curves of Rao's magnetoacoustic waves, depicting the imaginary (left panel) and real (right panel) parts of the frequency as functions of the wavenumber. Exact solutions (solid lines) and approximate solutions (dashed lines).

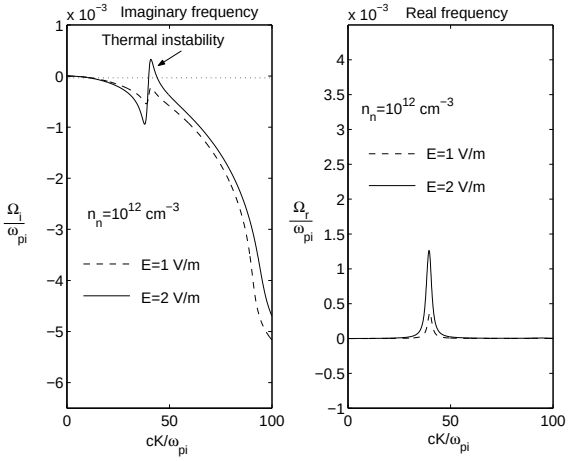

(b) Solutions of the nonlinear dispersion relation (1), depicting the imaginary part (left panel) and real part (right panel) of the frequency as functions of the wavenumber, for the electric pump field $E_0 = 1$ V/m (dashed lines) and $E_0 = 2$ V/m (solid lines).

Figure 2: Dispersion curves, weakly collisional plasma with $n_n = 10^{11}\,\mathrm{cm}^{-3}$.

s^{-1}, $\nu_{in} = 470\ \mathrm{s}^{-1}$, and $\tau_i = 1.3 \times 10^{-3}$ s.

In Figs. 1(a) and 2(a), we depict the dispersion curves for the modified Rao's magnetosonic waves, obtained by setting the left-hand side of Eq. (1) equal to zero. In Fig. 1(a), where we consider the weakly collisional case, we see the damping rates of the waves in the left panel and the real frequencies in the right panel. The propagating magnetosonic wave exhibits a cutoff $\Omega = \Omega_R \approx 1.5 \times 10^{-3}\,\omega_{pi}$ at $cK/\omega_{pi} = 0$, which is caused by the presence of dust. Next, we consider the strongly collisional case, depicted in Fig. 2(a), for which the damping rate is larger than the real frequency for the propagating wave. The imaginary and real parts of the frequencies are displayed in the left and right panels, respectively. The electromagnetic pump couples the two wave-modes to each other and to the electromagnetic sidebands, as described by the nonlinear dispersion relation (1). For sufficiently strong pump fields, the damped waves can be excited, as depicted in Figs. 1(b) and 2(b), where we display solutions of the dispersion relation, showing the imaginary and real parts of the low-frequency (left and right panels, respectively) as functions of the wavenumber cK/ω_{pi}. We investigated one case with the pump electric field amplitude $E_0 = 1$ V/m (dashed lines) and another case

with $E_0 = 2$ V/m (solid lines). In the weakly collisional case [Fig. 1(b)], both electric field amplitudes give rise to instabilities, as can be seen in the left panel where positive growth rates appear at wavenumber $cK/\omega_{pi} \approx 40$, which is twice the wavenumber of the pump wave. As can be seen in the right panel, this instability has a real part following the propagating Rao's wave mode for low wavenumbers ($cK/\omega_{pi} < 40$), and switches to a purely damped wavemode for high wavenumbers ($cK/\omega_{pi} > 40$). It can thus be attributed both to a parametric three-wave coupling between the electromagnetic pump wave and the propagating Rao's magnetosonic wave, and to a purely thermal instability where the electromagnetic pump wave couples to the purely damped wavemode of Rao's modified dispersion relation. In the strongly collisional case, depicted in Fig. 2(b), there exists an instability for the stronger pump field $E = 2$ V/m, but not for $E = 1$ V/m, as can be seen in the left panel. In this case, the real-valued dispersion curve follows the purely damped Rao's magnetosonic mode for both low and high wavenumbers, where the real part of the frequency vanishes (see the right panel); near $cK/\omega_{pi} \approx 40$, the real part of the frequency reaches the value of the propagating mode [cf. the right panel of Fig. 2(a)], which indicates that the propagating mode is important also for this case.

The numerical results can be interpreted as follows: In the ideal three-wave coupling between the electromagnetic pump wave and the propagating low-frequency wave, the electromagnetic wave scatters against the propagating wave, creating one slightly down-shifted counter-propagating electromagnetic daughter wave and one Rao's modified magnetosonic wave with approximately half the wavelength of the pump wave. In the coupling to the purely damped magnetoacoustic mode, the electromagnetic wave scatters against irregularities in the plasma and excites a counter-propagating daughter wave with the same frequency as the original wave. The original wave and the daughter wave create a standing-wave pattern. In the maxima of the standing waves, the plasma is heated locally. The heated plasma expands and reinforces the irregularities in the plasma, giving rise to a thermal instability where a grid pattern is created with a wavelength half of that of the pump wave.

This work was partially supported by the Deutsche Forschungsgemeinschaft (SFB 591) as well as by the Swedish Research Council (Contract No. 621-2001-2274).

[1] Rao, N. N., J. Plasma Phys. **317** (1995).
[2] Shukla, P. K., Eliasson, B. and Stenflo, L., J. Geophys. Res. **109**, A03301 (2004).